



Experimental study and cellular automaton simulation on solidification microstructure of Mg–Gd–Y–Zr alloy

Xu-Yang Wang, Fei-Fan Wang, Ke-Yan Wu, Xian-Fei Wang, Lv Xiao, Zhong-Quan Li, Zhi-Qiang Han*

Received: 2 November 2018 / Revised: 4 April 2019 / Accepted: 20 November 2019
© The Nonferrous Metals Society of China and Springer-Verlag GmbH Germany, part of Springer Nature 2019

Abstract The solidification microstructure of Mg–Gd–Y–Zr alloy was investigated via an experimental study and cellular automaton (CA) simulation. In this study, step-shaped castings were produced, and the temperature variation inside the casting was recorded using thermocouples during the solidification process. The effects of the cooling rate and Zr content on the grain size of the Mg–Gd–Y–Zr alloy were studied. The results showed that the grain size decreased with an increase in the cooling rate and Zr content. Based on the experimental data, a quantitative model for calculating the heterogeneous nucleation rate was developed, and the model parameters were determined. The evolution of the solidification microstructure was simulated using the CA method, where the quantitative nucleation model was used and a solute partition coefficient was introduced to deal with the solute trapping in front of the solid–liquid (S/L) interface. The simulation results of the grain size were in good agreement with the experimental data. The simulation also showed that the fraction of the eutectics decreased with an increasing cooling rate in the range of 2.6–11.0 °C·s⁻¹, which was verified indirectly by the experimental data.

Keywords Solidification microstructure; Mg–Gd–Y–Zr alloy; Cooling rate; Zr content; Nucleation; Cellular automaton

1 Introduction

Lightweight materials and processing technology have attracted considerable interest due to the need for energy conservation, emission reduction and environmental protection. As a lightweight structural material, magnesium alloy is widely used in automotive, aerospace and electronics industries [1–4]. Among various magnesium alloys, Mg–Gd–Y–Zr alloy has received immense attention in the aerospace field because of its high strength, excellent creep resistance and corrosion resistance at room and elevated temperatures [5, 6].

The characteristics of the castings in the aerospace field, such as a complex shape, large size and non-uniform thickness, lead to different cooling rates during the casting process. The cooling rate influences the solidification microstructure of the castings. Numerous studies have investigated the effect of the cooling rate on the solidification microstructure of Mg–Gd–Y–Zr alloy [7–9]. As reported, the grain size of the Mg–12.07Gd–3.27Y–0.38Zr alloy decreased when the cooling rate increased from 17.4 to 253.5 °C·s⁻¹, and the high cooling rate increased the solid solubility, which reduced the dendritic segregation of Gd and Y [10]. Pang et al. [11, 12] studied the effect of the cooling rate (from 0.7 to 3.6 °C·s⁻¹) on the solidification microstructure of the Mg–10Gd–3Y–0.5Zr alloy with a sand mold. The average grain size decreased from 59 to 39 μm. The content of the secondary phase increased from 17.6 vol% to 24.5 vol%, and the plate-shaped eutectic

X.-Y. Wang, F.-F. Wang, K.-Y. Wu, Z.-Q. Han*
School of Materials Science and Engineering, Tsinghua University, Beijing 100084, China
e-mail: zqhan@tsinghua.edu.cn

X.-Y. Wang, F.-F. Wang, K.-Y. Wu, Z.-Q. Han
Key Laboratory for Advanced Materials Processing Technology (Ministry of Education), Tsinghua University, Beijing 100084, China

X.-F. Wang, L. Xiao, Z.-Q. Li
Shanghai Spaceflight Precision Machinery Institute, Shanghai 201600, China

compound exhibited a continuous network instead of a coarsening discontinuous network when the cooling rate increased from 0.7 to 3.6 °C·s⁻¹. On the other hand, the Zr content, as a main nucleation agent, is important for controlling the grain size, thus affecting the mechanical properties in the as-cast Mg–Gd–Y–Zr alloys [13, 14]. Sun et al. [15, 16] reported that the grain size decreased, and the ultimate tensile strength (UTS) and elongation (EL) increased with an increasing Zr content from 0 wt% to 0.93 wt% in the Mg–10Gd–3Y alloy. Jiang et al. [17] found that the grain size decreased by approximately 50% when the Zr content increased from 0.3 wt% to 0.4 wt%, and they provided the relationship between the yield strength and grain size for the alloys with similar contents (Mg–10Gd–3Y–yZr, $y = 0.3, 0.4, \text{ and } 0.5$). The above-mentioned studies show that the grain size is mainly affected by the cooling rate and Zr content. However, these studies focused on the individual effect of the cooling rate or Zr content. The grain size is associated with the nucleation process. A quantitative nucleation model describing the effect of the cooling rate and Zr content on the nucleation rate is required, especially to simulate the microstructure. However, this type of nucleation model has rarely been reported.

Recently, with the development of computer technology and numerical simulation techniques, cellular automaton (CA) and phase field (PF) have become important and effective methods for simulating microstructure evolution in materials processing [18–28]. One of the most important tasks in the CA model is to calculate the kinetics of the solid–liquid (S/L) interface, which is associated with the solute partition at the S/L interface [29–33]. In an equilibrium solidification, the chemical potentials on either side of the interface remain equal, and the concentrations of the solid and liquid phases at the S/L interface follow the equation $k_e = C_s/C_l$, where k_e is the equilibrium partition coefficient and C_s and C_l are the concentrations of the solid and liquid phases, respectively. However, when the solidification velocity increases closely to the diffusion velocity, the Gd atom with a small diffusion coefficient could be caught by the solid phase, although there is a driving force for it to escape in the Mg–Gd–Y–Zr alloy. The actual ratio C_s/C_l deviates from k_e , and a transition from equilibrium segregation to solute trapping occurs [34, 35]. If the effect of the solidification velocity on the solute partition coefficient is ignored, the solute field cannot be solved accurately, and the fraction of the eutectics cannot be calculated accurately in the simulation.

In engineering practices, there is a strong demand for engineers to predict the characteristics of the microstructure, such as the grain size and content of the secondary phase. However, the models or simulation tools for

predicting the grain size and content of the secondary phase have not been established for the Mg–Gd–Y–Zr alloy. In this study, the effects of the cooling rate and Zr content on the grain size were studied experimentally. A quantitative model for calculating the heterogeneous nucleation rate of the Mg–Gd–Y–Zr alloy was developed based on the experimental data. The microstructure of the alloy was simulated using the CA method, where the nucleation model was used, and a solute partition coefficient was introduced to deal with the solute trapping in front of the S/L interface.

2 Experimental

2.1 Experiment procedure

The Mg–Gd–Y–Zr alloy was prepared using high-purity Mg (99.95 wt%) and master alloys, including Mg–25 wt% Gd, Mg–25 wt% Y and Mg–30 wt% Zr. The melting process was conducted in an electric resistance furnace under the mixed atmosphere of 1 vol% SF₆ + 99 vol% CO₂. The melt was refined at 750 °C for 5 min, cooled to 730 °C and poured into a permanent mold. Castings with five steps were produced, and thermocouples were used to record the temperature variation inside the castings during the solidification process. The geometry of the casting is shown in a previous study [7]. Samples for the optical microscope (OM, Zeiss Axio Scope A1) were taken from the temperature measurement point. The grain boundary for obtaining the data of the grain size should be identified. However, it is difficult to see the grain boundary in the OM image of the as-cast microstructure. The grain boundary could be observed clearly, if the samples were treated under the solution treatment at 500 °C for 6 h [36], and then they were corroded by 0.4 ml nitric acid and 20 ml anhydrous ethanol. The grain size was measured using a linear intercept technique referenced by ASTM Standard E 112-13.

2.2 Nucleation model

The aim of this section is to build a model which is capable of describing the heterogeneous nucleation during the solidification of the Mg–Gd–Y–Zr alloy based on the classical nucleation theory. A quantitative description of the nucleation process, incorporating the effects of the cooling rate and Zr content, is developed by determining the model parameters based on the experimental data. Christian [37] proposed the following equation for describing the heterogeneous nucleation rate (I_{hc}):

$$I_{\text{he}} = N_{\text{he}} \frac{k_{\text{B}}T}{h} \exp\left(-\frac{\Delta G_{\text{he}}^* + \Delta G_{\text{mo}}}{k_{\text{B}}T}\right), \quad (1)$$

where k_{B} is the Boltzmann constant; h is the Planck constant; T is the absolute temperature; ΔG_{mo} is the activation energy for diffusion; N_{he} is the number of atoms on the effective nucleus surface; and ΔG_{he}^* is the heterogeneous nucleation activation energy. Here, ΔG_{he}^* and N_{he} can be given as follows:

$$\Delta G_{\text{he}}^* = f(\theta)\Delta G^* \quad (2)$$

$$N_{\text{he}} = K_{\text{he}}N \quad (3)$$

where $\Delta G^* = \frac{\alpha\gamma^3T_0^2}{(\Delta h_0\Delta T)^2}$; γ is the surface tension; T_0 is the liquidus temperature; Δh_0 is the melting enthalpy in a unit volume; ΔT is the undercooling; and α is a factor that accounts for the shape of the nucleus ($\alpha = \frac{16\pi}{3}$ for the spherical nucleus). The parameter $f(\theta)$ is defined as the ratio of activation energies for heterogeneous and homogeneous nucleation; K_{he} is the heterogeneous nucleation coefficient, which can be determined based on the experimental data; and N is the number of atoms in a unit volume. The equation for describing the heterogeneous nucleation rate can be written as follows.

$$I_{\text{he}} = K_{\text{he}}N \frac{k_{\text{B}}T}{h} \exp\left(-\frac{\Delta G_{\text{mo}}}{k_{\text{B}}T}\right) \exp\left[-\frac{f(\theta)}{k_{\text{B}}T} \frac{\alpha\gamma^3T_0^2}{(\Delta h_0\Delta T)^2}\right] \quad (4)$$

The reasonable values of N and $\frac{k_{\text{B}}T}{h}$ for the general casting temperatures are $1 \times 10^{28} - 1 \times 10^{29} \text{ m}^{-3}$ and $1 \times 10^{13} \text{ s}^{-3}$, respectively. The parameter $K_{\text{he}}N \frac{k_{\text{B}}T}{h}$, as the coefficient to the exponential term, is evaluated as $1 \times 10^{42} K_{\text{ke}}$. The term $\frac{\alpha\gamma^3T_0^2f(\theta)}{(\Delta h_0)^2}$ is denoted by A_{θ} , and it is assumed that A_{θ} changes with $f(\theta)$. The above equation can be simplified as follows:

$$I_{\text{he}} = 10^{42} K_{\text{he}} \exp\left[-\frac{\Delta G_{\text{mo}} + A_{\theta}/(\Delta T)^2}{k_{\text{B}}T}\right] \quad (5)$$

Based on the assumption that the nucleation only occurs before the recalescence phenomenon in the solidification process, the grain density (n_{v}) can be obtained by the following equation:

$$n_{\text{v}} = \int_0^{\Delta T_{\text{max}}} \frac{I_{\text{he}}}{R_{\text{c}}} d\Delta T \quad (6)$$

where ΔT_{max} is the maximum undercooling, and R_{c} is the cooling rate. The nucleation rate is assumed to be a linear function of undercooling. Thus, Eq. (6) can be written as:

$$n_{\text{v}} = \frac{I_{\text{he}}^{\text{N}}}{2R_{\text{c}}} \Delta T_{\text{max}} \quad (7)$$

where I_{he}^{N} is the heterogeneous nucleation rate when the undercooling increases to ΔT_{max} .

The following equation is deduced by correlating Eqs. (5) and (7).

$$n_{\text{v}} = \frac{\Delta T_{\text{max}}}{2R_{\text{c}}} 10^{42} K_{\text{he}} \exp\left[-\frac{\Delta G_{\text{mo}} + A_{\theta}/(\Delta T_{\text{max}})^2}{k_{\text{B}}T}\right] \quad (8)$$

In the above equation, the proportion coefficient 0.5 can be incorporated into the heterogeneous nucleation coefficient (K_{he}), which is associated with Zr content in the Mg–Gd–Y–Zr alloy. Here, ΔG_{mo} and A_{θ} are assumed to be constants for the particular nucleation agent (Zr) in the Mg–Gd–Y–Zr alloy. The model parameters K_{he} , ΔG_{mo} and A_{θ} are determined by using the experimental data of n_{v} , ΔT_{max} and R_{c} .

2.3 Solute partition coefficient

In our previous study [38], a CA model was developed to simulate the morphology evolution of cast Mg alloys. In this model, the growth kinetics of dendrite was determined by the difference between the solute concentration based on the thermodynamics and the local compositions obtained by solving the solute transport equation. With this computational method, the solid fraction of the interfacial CA cells could be obtained. The solute partition coefficient plays an important role in solving the diffusion equation and calculating the variation of the solid fraction at the S/L interface. For the stable and metastable local equilibrium, the chemical potentials of the chemical elements across the interface must be equal for the liquid and solid phases. However, this condition is not obeyed when the solidification velocity increases closely to the diffusive velocity, and the solute partition coefficient cannot be calculated by $k_{\text{e}} = C_{\text{s}}/C_{\text{l}}$. Therefore, several models have been proposed to describe the dependence of the partition coefficient (k^*) on the solidification velocity. The most widely accepted model was proposed by Aziz [39]:

$$k^* = \frac{k_{\text{e}} + \delta_{\text{i}}V/D_{\text{i}}}{1 + \delta_{\text{i}}V/D_{\text{i}}} \quad (9)$$

where k_{e} is the equilibrium partition coefficient; δ_{i} is the atomic jump distance; D_{i} is the interfacial diffusion coefficient; and V is the solidification velocity. For $V = 0$, $k^* = k_{\text{e}}$, and for large $\delta_{\text{i}}V/D_{\text{i}}$, $k^* = 1$. It is difficult to acquire the values of D_{i} and δ_{i} ; therefore, the diffusion coefficient in the liquid phase (D_{L}) and the thickness of the diffusion layer in the liquid phase (δ_{L}) are used in Eq. (9).

3 Results and discussion

3.1 Experimental results

The castings of the Mg–10Gd–3Y–Zr alloys with Zr contents of 0.58 wt%, 1.26 wt% and 1.94 wt% were produced. In the solidification process, the cooling curves were recorded by thermocouples. The transient cooling rate, which is the first-order derivative of the cooling curve, varies with time. The transient cooling rate curve of the alloy can be divided into four stages. The first stage describes the cooling process of the liquid phase, in which the temperature of the melt decreases sharply. The second and third stages correspond to the solidification of the primary phase and the formation of the eutectics, respectively. In these two stages, the release of latent heat reduces the transient cooling rate. The transient cooling rate begins to increase after the melt has solidified completely in the last stage. Based on the above-mentioned characteristics, some parameters of solidification can be identified, as shown in Fig. 1. The parameter T_s is the starting temperature of nucleation of the primary phase, and t_s is the time corresponding to T_s . The parameter T_1 is the temperature immediately before recalescence, at which nucleation of the primary phase is assumed finished. T_{es} is the starting temperature of the eutectics; T_e is the ending temperature of solidification; and t_e is the time corresponding to T_e . The average cooling rate in the solidification process, which is denoted by R_c , was calculated using Eq. (10). Here, R_c is a unique parameter corresponding to a particular cooling curve or dT/dt curve. The cooling rate mentioned later in this paper represents the average cooling rate R_c .

$$R_c = (T_s - T_e)/(t_s - t_e) \quad (10)$$

The maximum undercooling (ΔT_{\max}) was calculated by Eq. (11).

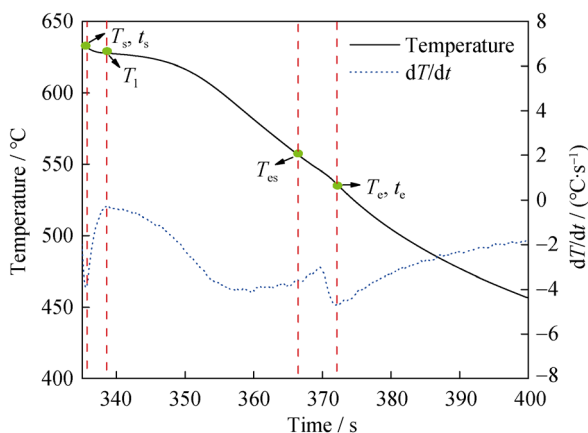


Fig. 1 Cooling curve and transient cooling rate curve (dT/dt) of Mg–Gd–Y–Zr alloy with 0.58 wt% Zr (when averaged cooling rate in solidification process being $2.6 \text{ }^\circ\text{C}\cdot\text{s}^{-1}$)

$$\Delta T_{\max} = T_s - T_1 \quad (11)$$

The maximum undercooling increases from 1.0 to $9.3 \text{ }^\circ\text{C}$ when the cooling rate increases from 2.6 to $11.0 \text{ }^\circ\text{C}\cdot\text{s}^{-1}$, according to Fig. 2, and the mathematic relation between the maximum undercooling and cooling rate can be expressed by the following equation.

$$\Delta T_{\max} = 0.99R_c - 1.57 \quad (12)$$

The OM images of the Mg–Gd–Y–Zr alloy with 0.58 wt% Zr at different cooling rates are shown in Fig. 3. Figure 4 shows the grain sizes of the Mg–Gd–Y–Zr alloys with various Zr contents at different cooling rates. The grain size of the Mg–Gd–Y–Zr alloy decreases with an increase in Zr content at the same cooling rate. When Zr content is 0.58 wt%, the grain size decreases from 73.94 to $50.10 \text{ }\mu\text{m}$ as the cooling rate changes from 2.6 to $6.7 \text{ }^\circ\text{C}\cdot\text{s}^{-1}$. A further increase in the cooling rate has little effect on the grain size. When the cooling rate increases from 3.0 to $8.8 \text{ }^\circ\text{C}\cdot\text{s}^{-1}$, the grain size of the Mg–Gd–Y–Zr alloy with 1.26 wt% Zr decreases from 49.04 to $42.26 \text{ }\mu\text{m}$. The grain size of the alloy with 1.94 wt% Zr decreases from 41.71 to $35.00 \text{ }\mu\text{m}$ with an increase in the cooling rate from 2.6 to $7.8 \text{ }^\circ\text{C}\cdot\text{s}^{-1}$.

3.2 Determination of parameters in nucleation model

The grain density was determined using the procedure provided in a previous study referenced by ASTM Standard E 112-85, where the grain size (l) is related to the grain density (n_v) as $n_v = 0.566l^{-3}$. The model parameters K_{he} , ΔG_{m0} and A_θ were determined by substituting the experimental data of n_v , ΔT_{\max} and R_c into Eq. (8), as listed in Table 1. Figure 5 shows the experimental results and the fitting results of the grain density. When the maximum undercooling increases, the grain density increases, and its

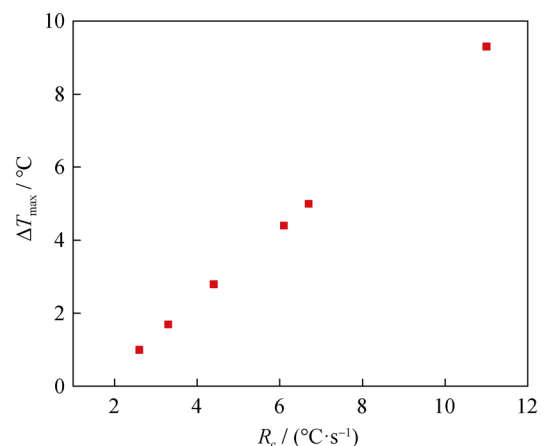


Fig. 2 Relationship between maximum undercooling (ΔT_{\max}) and cooling rate (R_c) of Mg–Gd–Y–Zr alloy with 0.58 wt% Zr

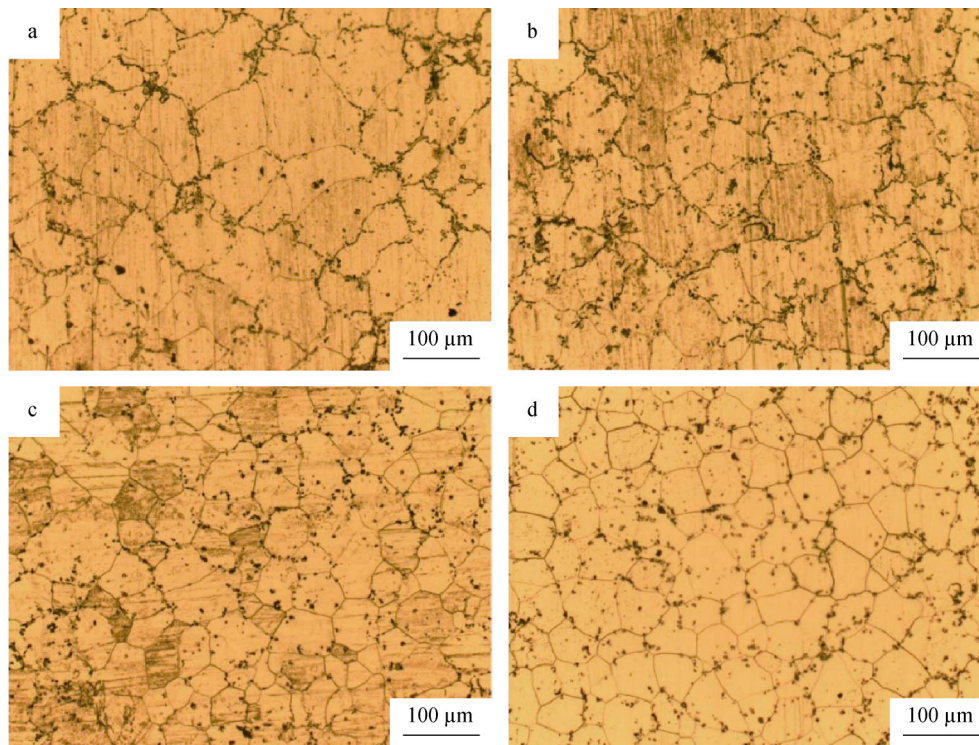


Fig. 3 OM images of Mg–Gd–Y–Zr alloy with 0.58 wt% Zr at various cooling rates: **a** 2.6 °C·s⁻¹, **b** 3.3 °C·s⁻¹, **c** 6.1 °C·s⁻¹ and **d** 11.0 °C·s⁻¹

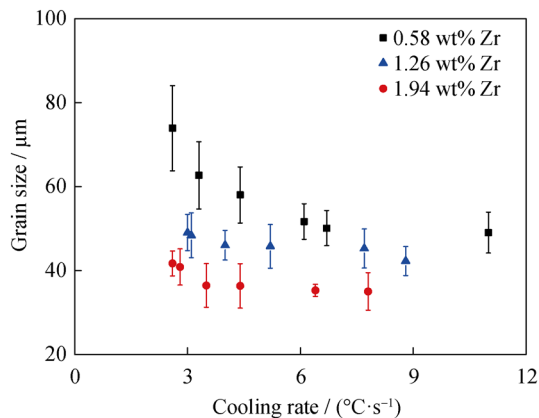


Fig. 4 Grain sizes of Mg–Gd–Y–Zr alloys with various Zr contents at different cooling rates

increasing rate decreases. At the same maximum undercooling, the grain density of the Mg–Gd–Y–Zr alloy with a high Zr content is higher than that of the alloy with a low Zr content. When the maximum undercooling changes from 3 to 6 °C, the increment of the grain density increases with an increase in Zr content.

3.3 Quantitative value of solute partition coefficient

During solidification of Mg–Gd–Y–Zr alloy, the primary phase precipitates from the liquid phase, which is followed

by the eutectic reaction. In the Mg–10Gd–3Y–Zr (0.58 wt%, 1.26 wt%, and 1.94 wt%) alloys, the contents of the main solute elements (Gd and Y) are higher than the nucleation agent (Zr). Wu et al. [7] proposed that the content of Gd in the secondary phase was higher than that in the primary phase, while the Y atoms uniformly distributed in the primary and secondary phases. It also means that Gd is easier to segregate due to its low diffusion coefficient. Therefore, the model of the binary alloy (Mg–Gd) could be applied to the CA program for simulating the solidification microstructure of the Mg–Gd–Y–Zr alloy.

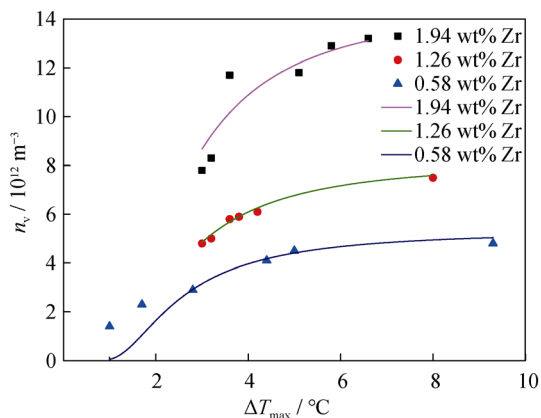
In the CA program, some parameters of the Gd atom for calculating the partition coefficient are listed in Table 2, and the solute partition coefficient of Gd can be calculated by Eq. (9). The solidification velocity was calculated by $v = \frac{l}{2t}$, where the growth time (t) was determined based on the cooling curve and dT/dt curve. Table 3 lists the results of the solute partition coefficient of the Mg–Gd–Y–Zr alloy with 0.58 wt% Zr. When the cooling rate increases from 2.6 to 11.0 °C·s⁻¹, the solute partition coefficient increases from 0.607 to 0.800.

3.4 Simulation results

The quantitative nucleation model that considered the effects of the cooling rate and Zr content on the grain size and the solute partition coefficient dealing with the solute

Table 1 Parameters in nucleation model

$\omega_{Zr}/\%$	$K_{ne}/10^{-14}$	$R_c/(\text{°C}\cdot\text{s}^{-1})$	$\Delta T_{max}/\text{°C}$	$n_v/10^{12} \text{ m}^{-3}$	$A_\theta/(\text{J}\cdot\text{°C})$	$\Delta G_{mo}/\text{J}$
0.58	2.8	2.6	1.0	1.4	3.12×10^{-20}	2.4×10^{-19}
		3.3	1.7	2.3		
		4.4	2.8	2.9		
		6.1	4.4	4.1		
		6.7	5.0	4.5		
1.26	4.3	11.0	9.3	4.8		
		3.0	3.0	4.8		
		3.1	3.2	5.0		
		4.0	3.6	5.8		
		5.2	3.8	5.9		
1.94	7.7	7.7	4.2	6.1		
		8.8	8.0	7.5		
		2.6	3.0	7.8		
		2.8	3.2	8.3		
		3.5	3.6	11.7		
		4.4	5.1	11.8		
		6.4	5.8	12.9		
		7.8	6.6	13.2		

**Fig. 5** Effects of maximum undercooling (ΔT_{max}) and Zr content on grain density (n_v)**Table 2** Parameters of Gd atom for calculating partition coefficient

Parameter	$D_L/(\text{m}^2\cdot\text{s}^{-1})$	δ/m	k_e
Value	3×10^{-11}	2×10^{-5}	0.28

trapping in the Mg–Gd–Y–Zr alloy was used in the CA simulation. Figure 6 shows the simulation results for the solidification microstructure of the Mg–Gd–Y–Zr alloy with 0.58 wt% Zr at various cooling rates. The average size of the secondary phase and the grain size decrease when the cooling rate increases from 2.6 to 6.1 $\text{°C}\cdot\text{s}^{-1}$. The

Table 3 Solidification velocity and partition coefficient at different cooling rates

$R_c/(\text{°C}\cdot\text{s}^{-1})$	$l/\mu\text{m}$	t/s	$v/(\mu\text{m}\cdot\text{s}^{-1})$	k^*
11.0	49.04	6.3	3.89	0.800
6.7	50.10	11.3	2.22	0.709
6.1	51.68	12.0	2.15	0.704
4.4	58.01	17.5	1.66	0.658
3.3	62.67	23.7	1.32	0.617
2.6	73.94	29.6	1.25	0.607

solute partition coefficient increases with an increase in the cooling rate; therefore, the distribution of the Gd content in the primary phase tends to be more homogeneous. Figure 7a, b shows the OM images which were also shown in our previous study [7]. Figure 7c, d shows the CA simulation results corresponding to Fig. 7a, b, respectively. The Gd content is not uniform from the center to the edge of the primary phase, low at the center, while high at the edge of the grain. With an increasing cooling rate, more Gd atoms are trapped in the solid phase, and the Gd content in the residual liquid phase decreases. Thus, the content of the secondary phase decreases.

Figure 8 shows the simulation results on the content of the eutectics in the Mg–Gd–Y–Zr alloy with 0.58 wt% Zr. The content of the eutectics calculated by CA method decreases with an increase in the cooling rate from 2.6 to

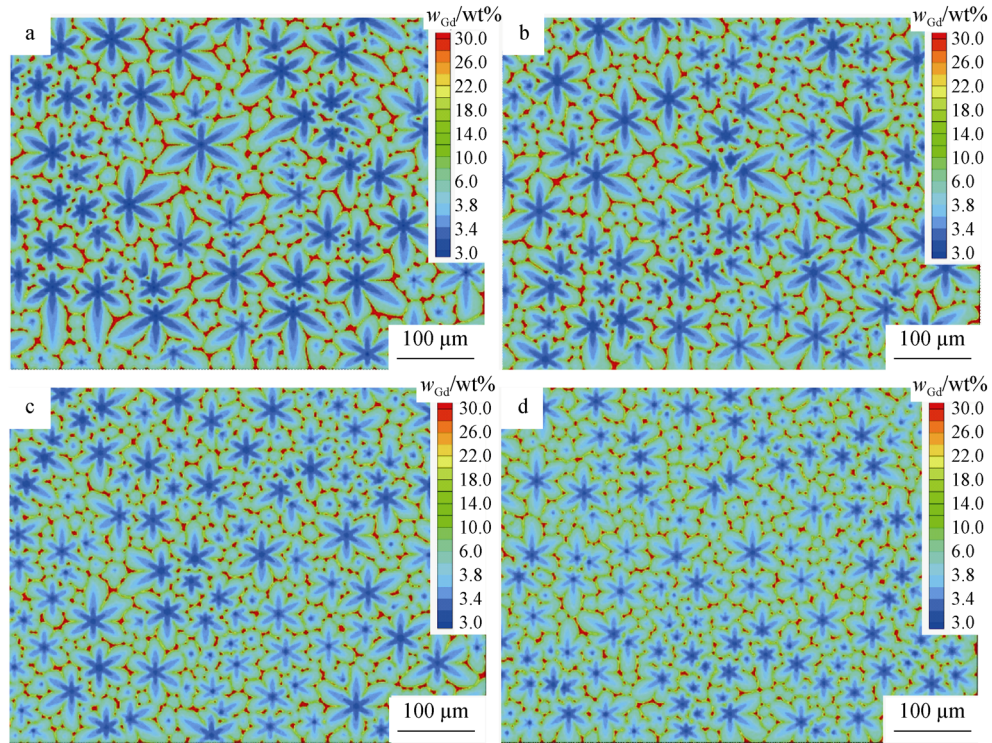


Fig. 6 Simulation results of Mg-Gd-Y-Zr alloy with 0.58 wt% Zr at various cooling rates: **a** $2.6\text{ }^{\circ}\text{C}\cdot\text{s}^{-1}$, **b** $3.3\text{ }^{\circ}\text{C}\cdot\text{s}^{-1}$, **c** $4.4\text{ }^{\circ}\text{C}\cdot\text{s}^{-1}$ and **d** $6.1\text{ }^{\circ}\text{C}\cdot\text{s}^{-1}$

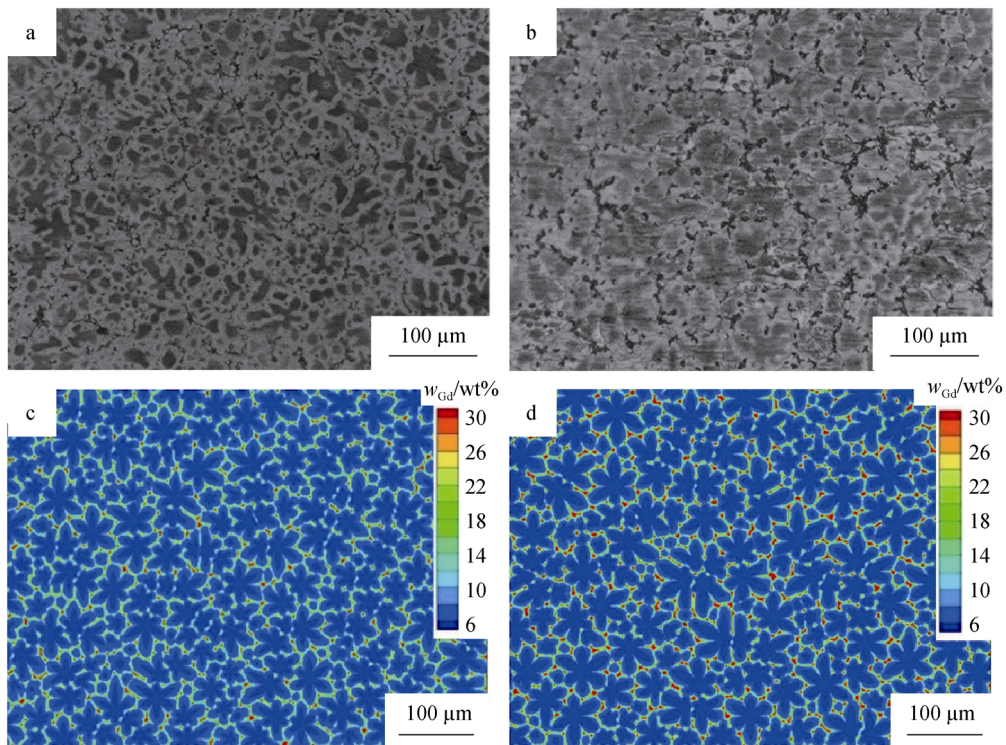


Fig. 7 OM images and simulation results of Mg-Gd-Y-Zr alloy with 0.58 wt% Zr at different cooling rates: **a** experimental result at $11.0\text{ }^{\circ}\text{C}\cdot\text{s}^{-1}$ [7], **b** experimental result at $6.7\text{ }^{\circ}\text{C}\cdot\text{s}^{-1}$ [7], **c** simulation result at $11.0\text{ }^{\circ}\text{C}\cdot\text{s}^{-1}$, and **d** simulation result at $6.7\text{ }^{\circ}\text{C}\cdot\text{s}^{-1}$

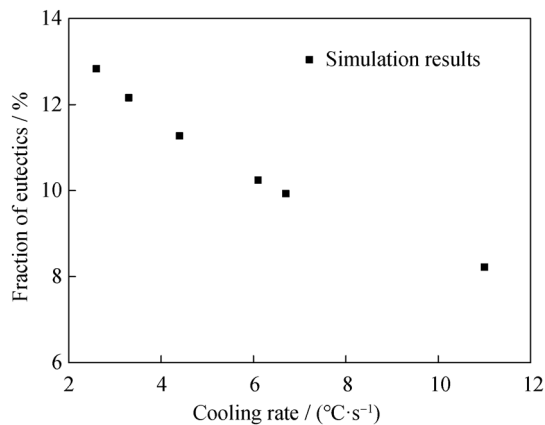


Fig. 8 Simulation results on fraction of eutectics

11.0 °C·s⁻¹. As shown in our previous study [7], the experimental results for the content of the secondary phase decrease with an increase in the cooling rate from 2.6 to 11.0 °C·s⁻¹. The eutectics is composed of α -Mg and the secondary phase; thus, the experimental data of the content of the secondary phase can be used to qualitatively verify the simulation results for the content of the eutectics.

4 Conclusion

In this study, the solidification microstructure of the Mg–Gd–Y–Zr alloy was investigated via an experimental study and a CA simulation. The grain size of the Mg–Gd–Y–Zr alloy decreases with an increasing Zr content at the same cooling rate. When the cooling rate increases from 2.6 to 6.7 °C·s⁻¹, the grain size of the Mg–Gd–Y–Zr alloy with 0.58 wt% Zr decreases from 73.94 to 50.10 μm . When the cooling rate increases from 3.0 to 8.8 °C·s⁻¹, the grain size of the alloy with 1.26 wt% Zr decreases from 49.04 to 42.26 μm . When the cooling rate increases from 2.6 to 7.8 °C·s⁻¹, the grain size of the alloy with 1.94 wt% Zr decreases from 41.71 to 35.00 μm . Based on the experimental data, a quantitative nucleation model describing the effects of the cooling rate and Zr content on the heterogeneous nucleation rate of the Mg–Gd–Y–Zr alloys was developed and the model parameters were determined. The solidification microstructure was simulated using the CA method, where the nucleation model was used and a solute partition coefficient was introduced to deal with solute trapping in front of the S/L interface. The simulation results of the grain size were in a good agreement with the experimental data. The simulation also shows that the fraction of the eutectics decreases with an increasing cooling rate in the range of 2.6–11.0 °C·s⁻¹, which is verified indirectly by the experimental data.

Acknowledgements This study was financially supported by the National Key Research and Development Program of China (No. 2016YFB0701204), the National Science and Technology Major Project of China (No. 2017ZX04006001) and the National Natural Science Foundation of China (No. U1737208).

References

- [1] Liu H, Ju J, Yang XW, Li YH, Jiang JH, Ma AB. Microstructure and mechanical property of Mg–10Gd–2Y–1.5 Zn–0.5 Zr alloy processed by eight-pass equal-channel angular pressing. *Rare Met.* 2018. <https://doi.org/10.1007/s12598-018-1022-1>.
- [2] Zhang K, Li X, Li Y, Yuan J, Liu X, Wang S. Properties of ZM51 magnesium alloys with heat treatments. *Chin J Rare Met.* 2019;43(6):585.
- [3] Han Z, Pan H, Li Y, Luo AA, Sachdev AK. Study on pressurized solidification behavior and microstructure characteristics of squeeze casting magnesium alloy AZ91D. *Metall Mater Trans B.* 2015;46(1):328.
- [4] Han GM, Han ZQ, Luo AA, Liu BC. Microstructure characteristics and effect of aging process on the mechanical properties of squeeze-cast AZ91 alloy. *J Alloys Compd.* 2015;641:56.
- [5] Zheng L, Liu C, Wan Y, Yang P, Shu X. Microstructures and mechanical properties of Mg–10Gd–6Y–2Zn–0.6Zr (wt%) alloy. *J Alloys Compd.* 2011;509(35):8832.
- [6] Xu C, Xu SW, Zheng MY, Wu K, Wang ED, Kamado S, Wang GJ, Lv XY. Microstructures and mechanical properties of high-strength Mg–Gd–Y–Zn–Zr alloy sheets processed by severe hot rolling. *J Alloys Compd.* 2012;524:546.
- [7] Wu K, Wang X, Xiao L, Li Z, Han Z. Experimental study on the effect of cooling rate on the secondary phase in as-cast Mg–Gd–Y–Zr alloy. *Adv Eng Mater.* 2018;20(3):1700717.
- [8] Xu C, Zheng MY, Wu K, Wang ED, Fan GH, Xu SW, Kamado S, Liu XD, Wang GJ, Lv XY. Effect of cooling rate on the microstructure evolution and mechanical properties of homogenized Mg–Gd–Y–Zn–Zr alloy. *Mater Sci Eng, A.* 2013;559:364.
- [9] Huo L, Han ZQ, Liu BC. Effect of microstructure on tensile and fatigue properties of cast Mg–10Gd–2Y–0.5Zr alloy. *Int J Cast Met Res.* 2009;22(1–4):123.
- [10] Zhou J, Yang Y, Tong W, Wang J, Fu J, Wang B. Effect of cooling rate on the solidified microstructure of Mg–Gd–Y–Zr alloy. *Rare Metal Mater Eng.* 2010;39(11):1899.
- [11] Pang S, Wu G, Liu W, Sun M, Zhang Y, Liu Z, Ding W. Effect of cooling rate on the microstructure and mechanical properties of sand-casting Mg–10Gd–3Y–0.5Zr magnesium alloy. *Mater Sci Eng, A.* 2013;562:152.
- [12] Pang S, Wu G, Liu WC, Zhang L, Zhang Y, Conrad H, Ding WJ. Influence of cooling rate on solidification behavior of sand-cast Mg–10Gd–3Y–0.4Zr alloy. *Trans Nonferrous Met Soc China.* 2014;24(11):3413.
- [13] Lee YC, Dahle AK, StJohn DH. The role of solute in grain refinement of magnesium. *Metall Mater Trans A.* 2000;31(11):2895.
- [14] Qian M, Das A. Grain refinement of magnesium alloys by zirconium: formation of equiaxed grains. *Scr Mater.* 2006;54(5):881.
- [15] Sun M, Wu G, Wang W, Ding W. Effect of Zr on the microstructure, mechanical properties and corrosion resistance of Mg–10Gd–3Y magnesium alloy. *Mater Sci Eng, A.* 2009;523(1–2):145.
- [16] Sun M, Easton MA, StJohn DH, Wu G, Abbott TB, Ding W. Grain refinement of magnesium alloys by Mg–Zr master alloys:

- the role of alloy chemistry and Zr particle number density. *Adv Eng Mater.* 2013;15(5):373.
- [17] Jiang L, Liu W, Wu G, Ding W. Effect of chemical composition on the microstructure, tensile properties and fatigue behavior of sand-cast Mg–Gd–Y–Zr alloy. *Mater Sci Eng, A.* 2014;612:293.
- [18] Zhang X, Zhao J, Jiang H, Zhu M. A three-dimensional cellular automaton model for dendritic growth in multi-component alloys. *Acta Mater.* 2012;60(5):2249.
- [19] Wu M, Xiong S. Microstructure simulation of high pressure die cast magnesium alloy based on modified CA method. *Acta Metall Sin.* 2010;46(12):1534.
- [20] Su B, Han Z, Liu B. Cellular automaton modeling of austenite nucleation and growth in hypoeutectoid steel during heating process. *ISIJ Int.* 2013;53(3):527.
- [21] Han G, Han Z, Luo AA, Liu B. Three-dimensional phase-field simulation and experimental validation of β -Mg17Al12 phase precipitation in Mg–Al-based alloys. *Metall Mater Trans A.* 2015;46(2):948.
- [22] Han Z, Han G, Luo AA, Liu B. Large-scale three-dimensional phase-field simulation of multi-variant β -Mg17Al12 in Mg–Al-based alloys. *Comput Mater Sci.* 2015;101:248.
- [23] Beltran-Sanchez L, Stefanescu DM. Growth of solutal dendrites—a cellular automaton model. *Int J Cast Met Res.* 2003;15(3):251.
- [24] Beltran-Sanchez L, Stefanescu DM. Growth of solutal dendrites: a cellular automaton model and its quantitative capabilities. *Metall Mater Trans A.* 2003;34(2):367.
- [25] Han G, Han Z, Luo AA, Sachdev AK, Liu B. A phase field model for simulating the precipitation of multi-variant β -Mg17Al12 in Mg–Al-based alloys. *Scripta Mater.* 2013;68(9):691.
- [26] Yin H, Felicelli SD. A cellular automaton model for dendrite growth in magnesium alloy AZ91. *Model Simul Mater Sci Eng.* 2009;17:75011.
- [27] Zhang L, Wang YM, Zhang CB, Wang SQ, Ye HQ. A cellular automaton model of the transformation from austenite to ferrite in low carbon steels. *Model Simul Mater Sci Eng.* 2003;11:791.
- [28] Michelic SC, Thuswaldner JM, Bernhard C. Polydimensional modelling of dendritic growth and microsegregation in multi-component alloys. *Acta Mater.* 2010;58(7):2738.
- [29] Zhu MF, Cao W, Chen SL, Hong CP, Chang YA. Modeling of microstructure and microsegregation in solidification of multi-component alloys. *J Phase Equilib Diffus.* 2007;28(1):130.
- [30] Luo S, Zhu MY. A two-dimensional model for the quantitative simulation of the dendritic growth with cellular automaton method. *Comput Mater Sci.* 2013;71:10.
- [31] Zhao Y, Qin RS, Chen DF. A three-dimensional cellular automata model coupled with finite element method and thermodynamic database for alloy solidification. *J Cryst Growth.* 2013;377:72.
- [32] Sobolev SL. Rapid solidification under local nonequilibrium conditions. *Phys Rev E.* 1997;55(6):6845.
- [33] Pineau A, Guillemot G, Tournet D, Karma A, Gandin CA. Growth competition between columnar dendritic grains—cellular automaton versus phase field modeling. *Acta Mater.* 2018;155:286.
- [34] Wang H, Liu F, Yang W, Chen Z, Yang G, Zhou Y. Solute trapping model incorporating diffusive interface. *Acta Mater.* 2008;56(4):746.
- [35] Hillert M. Solute drag, solute trapping and diffusional dissipation of Gibbs energy. *Acta Mater.* 1999;47(18):4481.
- [36] Liu Y, Xiao L, Zou W, Li B. Optimization of mechanical properties of GW63K heat-resistant Mg alloy. *Hot Work Technol.* 2015;24:210.
- [37] Christian JW. *The Theory of Transformation in Metals and Alloys.* 2nd ed. Oxford: Pergamon Press; 1975. 624.
- [38] Huo L, Han Z, Liu B. Modeling and simulation of microstructure evolution of cast magnesium alloys using CA method based on two sets of mesh. *Acta Metall Sin.* 2009;45(12):1414.
- [39] Aziz MJ. Model for solute redistribution during rapid solidification. *J Appl Phys.* 1982;53(2):1158.